

# ELECTROMAGNETIC MODELING OF FAST BEAM CHOPPER FOR SNS PROJECT\*

S.S. Kurennoy

Los Alamos National Laboratory, Los Alamos, NM 87545, USA

## Abstract

High current and stringent restrictions on beam losses in the designed linac and storage ring for the Spallation Neutron Source (SNS) require clean and fast – with the rise time from 2% to 98% less than 2.5 ns – beam chopping in the linac front end, at the beam energy 2.5 MeV. The development of new traveling-wave deflecting current structures, based on meander lines, for the SNS fast chopper is discussed. Three-dimensional time-domain computer simulations with MAFIA are used to study transient effects in the chopper and to optimize current structure design.

## 1 SNS CHOPPER SYSTEM

The SNS is a next-generation pulsed spallation neutron source designed to deliver 1 MW of beam power on the target at 60 Hz in its initial stage [1,2]. It will consist of a 1-GeV linear  $H^-$  accelerator and an accumulator ring. The SNS storage ring accumulates the linac beam during a few hundred turns (a macropulse, about 1 ms) using  $H^-$  injection through a carbon foil. The beam injected into the ring is stacked into a single long bunch, and the linac macropulse must be chopped at near the ring revolution frequency 1.188 MHz to provide a gap required for the kicker rise time during a single-turn ring extraction. The final clean beam chopping in the linac is to be done in the Medium Energy Beam Transport (MEBT) line.

The MEBT transports 28 mA of peak beam current from a 2.5-MeV 402.5-MHz RFQ to a drift-tube linac. A 0.5-m space is allocated for the chopper that deflects the beam into a beam stop during the 35% beam-off time. The chopper parameters are summarized in Table 1.

Table 1: MEBT Chopper Specifications

Parameter	Value	Comment
Beam energy	2.5 MeV	$\beta=0.073$
Length	$\leq 0.5$ m	shorter is better
Gap	$\geq 1$ cm	adjustable
Pulser voltage	$\pm 900$ V	currently achievable with FETs
Deflection angle	18 mrad	
Chopping period	841 ns	
Duty factor	35 %	65 % beam on
Rise / fall time	$< 2.5$ ns	2–98 % (final goal)

To mitigate the effects of a partial chopping or small errors in the timing system, an identical “anti-chopper” will be placed in the MEBT line at an optically symmetric point from the chopper to return uncollimated beam to the axis. The preliminary chopping stage in the Low Energy Beam Transport (LEBT) line, at 100 keV, see [2], is introduced to reduce the beam power deposited at the MEBT beam stop. While the LEBT electrostatic chopper system has much slower rise and fall times (tens of ns) than the MEBT one, it is easier to absorb the bulk of the chopped beam at the low LEBT energy.

At any given moment as the beam passes through the MEBT chopper, there are about ten bunches along the chopper length. Even with an “ideal” pulse generator, the only way to avoid partially chopped bunches is to apply a traveling-wave current structure. The deflecting electric-field pulse fills the chopper with the phase velocity along the beam path matching the beam velocity and propagates together with the beam. The bunches following the pulse front are fully deflected while those ahead of the front are not disturbed. Providing the field-pulse front (and its end) shorter than the bunch-to-bunch spacing (2.5 ns, or about 5 cm) is the most challenging requirement to the chopper system. As an initial goal, the rise/fall time below 5 ns is acceptable; it will lead to one partially chopped bunch at the front and the end of each chopper pulse.

## 2 CHOPPER CURRENT STRUCTURE

### 2.1 Coax-to-plate LANSCE chopper

A traveling-wave chopper for  $H^\pm$  beams at 750 keV [3] has been working successfully for many years at LAMPF (now LANSCE) in Los Alamos. It provides the rise time of about 7 ns, mostly due to the pulse modulator. The coax-plate current structure itself is capable of providing a pulse front about 2-3 ns with an overshoot on the 10% level ringing for a few ns. The 1-m long structure consists of two parallel plates, each interfaced with many small strip segments connected with coaxial cables on the reverse side of each plate to form a continuous circuit along the structure, see Fig.1.

The voltages on the upper and lower plates are synchronized and have opposite signs so that the resulting vertical electric field deflects the beam that travels between the plates. The structure rise and fall time limita-

\* Work supported by the US Department of Energy.

tions are caused by stray capacitance between the segments and by multiple coax-to-segment transitions.



Figure 1: Photograph of traveling-wave current structure used in the LANSCE beam chopper.

## 2.2 Meander-line current structure

A new current structure based on a meander line with separators (Fig.2) has been proposed [4]. A strip transmission line forms the meander, which works as a slow-wave structure. The strip itself can be either straight or notched, as the one shown in Fig.2.

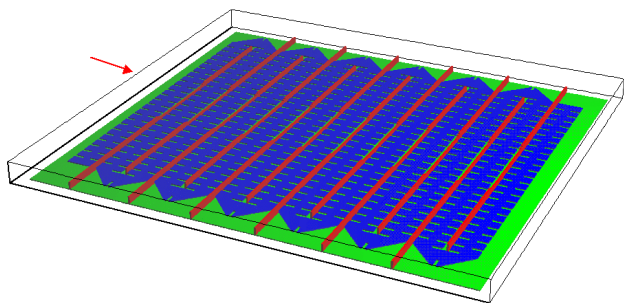


Figure 2: 1/4-length MAFIA model of meander current structure: notched meander strip line (blue) above the ground plate (green) with separators (red), cf. Fig.3. Only the lower plate is shown. The arrow indicates the beam path in the upper plane of the box drawn.

The line parameters are adjusted to provide the line characteristic impedance  $50 \Omega$ . The meander bends are chamfered to avoid pulse reflections. The separators (or guard barriers) rising from and electrically connected to the ground plane are used to reduce the coupling between the adjacent sections of the meander line, see in Fig.3. The new design has no multiple coax-to-plate transitions and is easier for manufacturing.

A proper ratio of the meander period to its width provides the required phase velocity of the voltage pulse,  $v = \beta c$ , along the beam direction. For a straight strip, the meander width transverse to the beam is simply  $b = (w+g)(1/\beta-1)$ , where  $w$  is the strip width and  $g$  is the gap width between the adjacent strips.

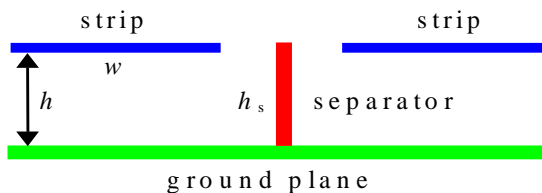


Figure 3: A partial vertical cut in the beam path plane of the meander current structure: the separator is inserted between two adjacent pieces of the transmission line.

3-D time-domain modeling with the electromagnetic simulator MAFIA [5] has been used to study transient effects in the current structure. The simulations [4] used MAFIA version 3.20 package. Essentially, it was done similar to S-parameter calculations: the strip TEM wave was loaded into the structure, and the voltages and the electric fields on the beam path were recorded as it propagated along the chopper. This approach required additional calculations of the 2-D eigenmodes at the entrance and exit ports. And these ports themselves had to be artificially introduced to simulate waveguides connected to the structure. The time dependence of the TEM-wave amplitude can be chosen as required. We used either harmonic signals at a fixed frequency to analyze frequency response, or step-function pulses to study the rise and fall times. In the last case the step was smoothed by  $\sin^2$  for about 0.1 ns to filter out very high frequencies. The same smoothing was applied to finite-length pulses.

It was shown [4] that even without separators, the meander structure has a rise time 2–2.5 ns; with separators it can be reduced down to 1–1.25 ns, depending on the separator height, see Fig.4. The structure fall time was found to be about the same as the rise time. High separators, however, reduce the effective field on the beam path by 10–20% depending on their height  $h_s$ , cf. Fig.4.

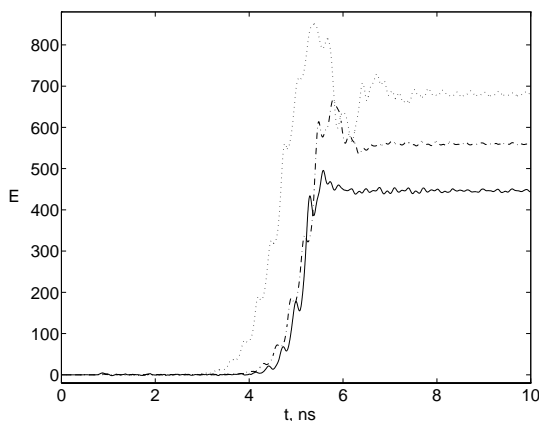


Figure 4: Vertical electric field, in arbitrary units, at a fixed point on the beam path versus time in the half-length meander structure with separators  $h_s = 2h$  (solid),  $h_s = h$  (dash-dotted), and without them (dotted). The voltage amplitude is the same for all cases.

### 2.3 Simple prototype test

To check our simulation results, a very simple model structure with a straight-strip meander line on a printed-circuit board (PCB) has been manufactured at LANL. The PCB with the meander on its bottom surface was placed on 1.25-mm barriers-separators sticking out of the aluminum ground plane, see Fig.5. The prototype length is 12.5 cm. Obviously, the presence of the dielectric introduces some additional dispersion, and it will stretch the voltage pulse front and end. Nevertheless, this prototype was chosen because of manufacturing simplicity.

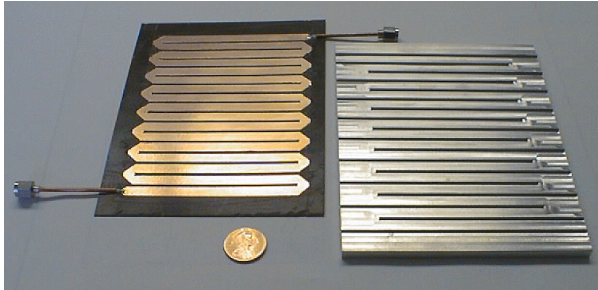


Figure 5: Photograph of the prototype structure: straight-strip meander line on PCB (left) and ground plate with separators (right).

Corresponding MAFIA time-domain simulations have been performed for the prototype structure taking into account the dielectric properties of the PCB material. The transient effects in the prototype have been measured with a TDR and were found to agree well with the MAFIA calculations, with all transitions within a 2-ns range, see Fig.6. Some small differences in the pulse shape in two pictures are due to stronger high-frequency components (tens of GHz) in calculation results. Clearly, these very high frequencies have been filtered out in the experimental setup by wires and connections.

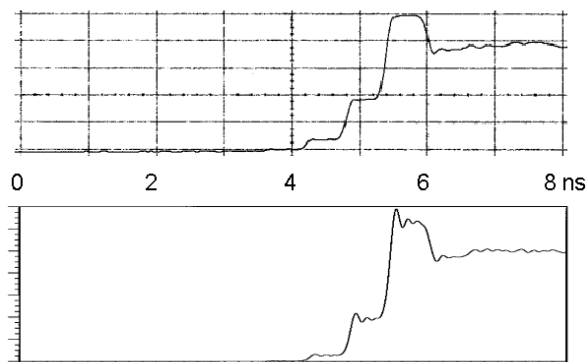


Figure 6: The voltage pulse front in the prototype structure: TDR measurements (top) and MAFIA simulations (bottom).

### 2.4 Notched-strip meander line

Our early work [4] dealt mostly with straight-strip meander structures. Using a notched strip line in the meander instead of a straight one has some advantages. First, the notches provide an additional inductive load that slows down the wave along the strip. A notch of depth  $d$  and width  $a \leq h$  adds the inductance  $L_1 = (\pi/2)\mu_0 h d^2 / w^2$  [6]. In a first approximation, the capacitance per unit length  $C'$  remains the same as for the straight strip, i.e.  $C' \approx C'_0 = \epsilon_0 w / h$ , while the inductance increases from  $L'_0 = \mu_0 h / w$  to  $L' = \mu_0 h / w + 2L_1 / p$ , where  $p$  is the notch spacing period. Then we estimate the phase velocity  $v_{ph} = 1 / (L' C')^{1/2}$  and adjust the impedance  $Z = (L' / C')^{1/2}$  to be  $50 \Omega$ . The ratio  $v_{ph} / c \approx (L'_0 / L')^{1/2}$  depends on the notch depth and the number of notches per unit length. For example, the TEM wave propagates along the notched strip shown in Fig.2 and Fig.7 with the phase velocity about  $0.75c$ .

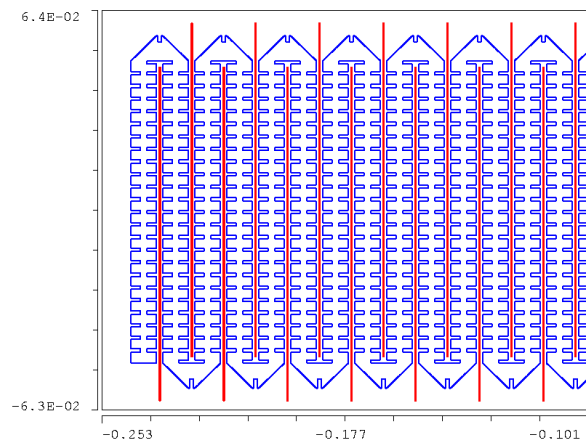


Figure 7: One quarter of the full-length MAFIA model for the notched-strip meander current structure with separators (red lines): 2-D cross section in the strip plane, cf. Fig.2. All dimensions are in meters.

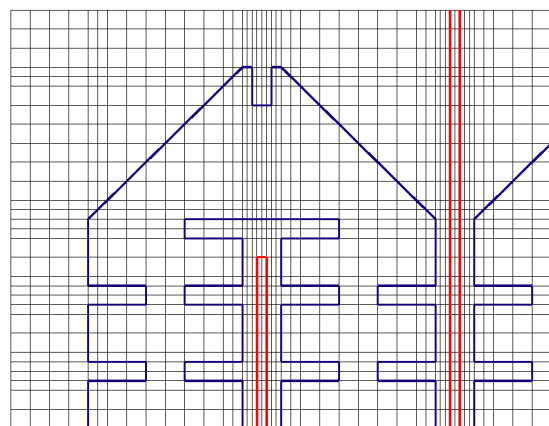


Figure 8: Details of Fig.7 (upper left corner) with mesh lines shown.

As a result, we need a smaller number of bends in the notched-strip meander and can use wider strips for a fixed meander width. The larger ratio of the strip width  $w$  to the strip-to-strip gap width  $g$  increases the structure field efficiency. For the meander in Fig.7, the notched-strip width  $w$  is 8 mm compared to 5 mm for a straight line. The meander width transverse to the beam is about 11 cm,  $h=1$  mm and  $g=2$  mm in both cases. In addition, the notches also reduce the magnetic coupling between adjacent strips since the wave magnetic field is concentrated closer to the strip center. Our recent efforts [7,8] have been directed toward optimizing the notched-strip design.

In modeling the full-length structure, the detailed mesh – like the one in Fig.8 – included up to 3 millions mesh points. Most of our MAFIA computations have been performed on SUN workstations Ultra-1 and Ultra-2. In earlier simulations [4] with MAFIA 3.20 we needed to load a pre-calculated TEM-mode into the structure. The MAFIA version 4 [5] allows simply to feed the strip with a voltage from a filament with some RLC-parameters, which connects the strip to the ground plate. The voltage can be an arbitrary function of time. We have used voltages profiled as either step-functions (smoothed by  $\sin^2$  to filter out very high frequencies) or as finite-length pulses. As the voltage pulse propagates along the structure, the electric field on the beam path is recorded. As an example, Fig.9 shows the deflecting field created by a voltage pulse with 1-ns  $\sin^2$  front, flat top at 1 kV for 3 ns, and 1-ns  $\sin^2$  end, in the full-length 50-cm model of the type shown in Figs. 2, 7 and 8. Such a pulse would kick out exactly two linac bunches.

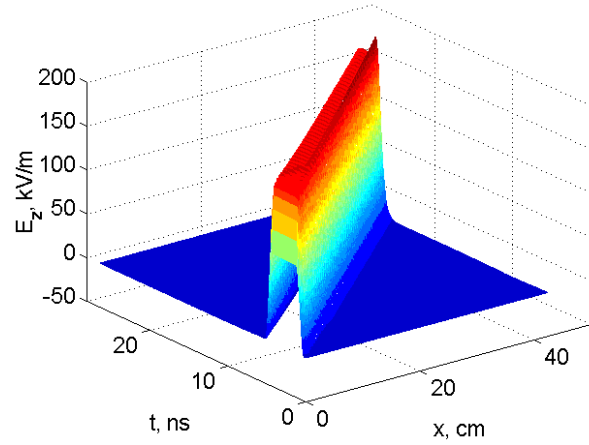


Figure 9: Deflecting field on the beam path versus time and position in the notched-strip meander structure for a 1-3-1-ns 1-kV driving pulse.

As the pulse propagates, its shape is slightly distorted by developing an overshoot. However, the pulse front and end both remain well within 2-ns range, see also Fig.10.

Cross-sections of the surface plot in Fig.9 for a given position  $x$  along the structure show the time dependence of the field at this location, see Fig.10, left. The development of the overshoot is clearly visible for the pulse in the middle and near the structure end. Straight-strip meanders produce slightly larger pulse distortions [7], as one can see in Fig.10, right. The same driving voltage pulse was used for simulations in both cases. Comparison of the pulse amplitudes in Figs.10 (also Figs. 11) confirms that the notched-strip meander provides slightly higher field efficiency than the straight-strip one.

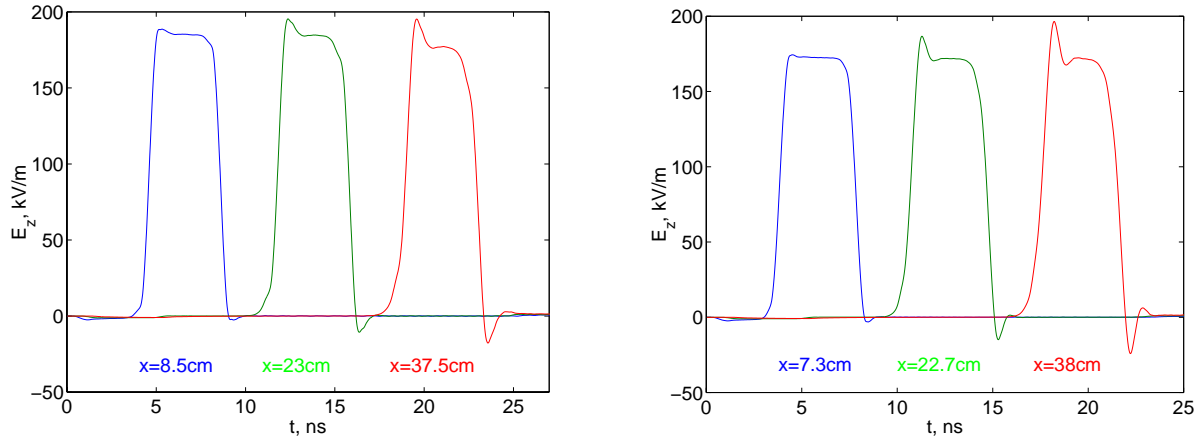


Figure 10: Deflecting field versus time in 3 different points on the beam path in the notched-strip (left) and straight-strip (right) meander structures.

Cross-sections of Fig.9 taken at given time  $t$  produce snapshots of the deflecting field as shown in Fig.11, left. Small wiggles on the pulse tops are due to differences of the field in points above the middle of the strip and above the separators. In fact, these field variations will even

help to spread the deflected beam slightly on the beam stop. A similar picture for the straight-strip meander is plotted in Fig.11, on the right side. The number of wiggles in this case is larger because the structure has a

shorter period along the beam axis,  $w+g=7\text{mm}$ , compared to 10 mm for the notched-strip meander.

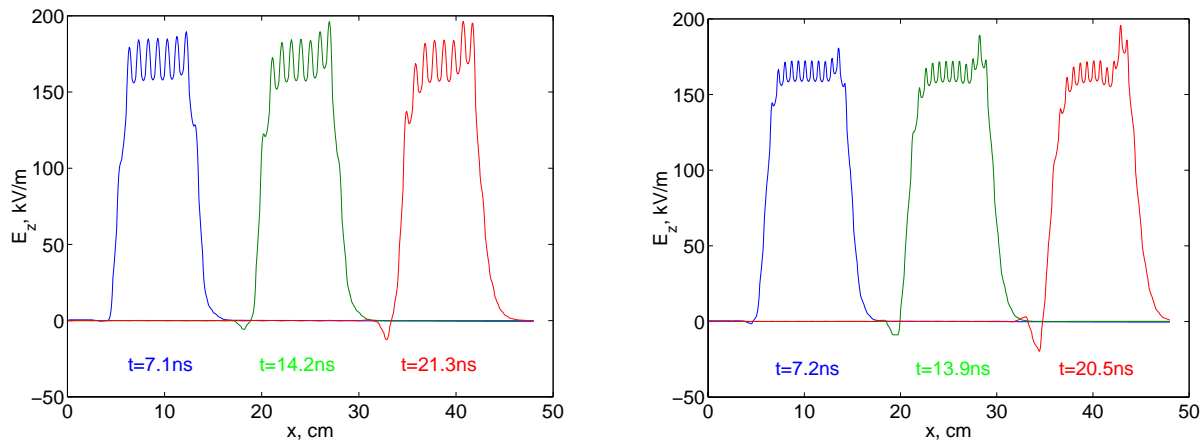


Figure 11: Snapshots of the deflecting field on the beam path in the notched-strip meander structure (left), cf. Fig.9, and in the straight-strip meander structure (right).

While Fig.11 presents only three “snapshots” of the field pulse shape, it is relatively easy to produce a movie showing how the pulse propagates along the structure. It can be done by recording a large number (a few hundred) of frames – similar to those in Fig.11 – separated by short time intervals. The MAFIA postprocessor provides such an option for video recording; however, the corresponding movie file is extremely large. We found a more convenient way to keep this information: recording the MAFIA movie from the screen (we use an X-windows emulator on PC) with a simple PC utility Hypercam produces a very compact avi-file, which can be played later with any media player.

Our design optimization [7,8] leads to the notched-meander structure shown in Figs.2, 7 and 8. Starting from initial analytical estimates for the geometrical parameters, we used MAFIA simulations to adjust the line characteristic impedance and the pulse phase velocity along the beam. The notches are 3-mm deep, 1-mm wide, and spaced by 4 mm. Additional 2-mm deep notches on the bends have been introduced to eliminate pulse reflections. To increase the effective field on the beam path without increasing the rise time, the profiled separators have been introduced: they are low (i.e., flush with the strip line) in the middle, near the beam axis, and higher near the sides, see Figs.2-3.

### 3 CONCLUSIONS

A new current structure based on a meander line has been developed. The 3-D time-domain modeling shows that the structure is capable to provide the rise and fall times on the order of 1 ns. Further simulations will include more engineering details like mechanical supports, as well as beam dynamics and PIC-simulations. Manufacturing of the full-length prototypes and their measurements are also planned.

The voltage generator development for this fast chopper remains an important and challenging issue. We will proceed with the proof-of-principle pulser design using currently available technology, while continuing to work with manufacturers on development of faster powerful FETs.

### 4 ACKNOWLEDGEMENTS

The author would like to thank John Power, who performed measurements of the prototype and contributed a lot to its manufacturing. Thanks to Glen Lambertson for suggesting the use of a notched strip in the transmission line. Useful discussions with Andy Jason and Frank Krawczyk are gratefully acknowledged.

### REFERENCES

- [1] B.R. Appleton et al., *Proceed. of EPAC (Barcelona, 1996)*, p.575. – IOP Publishing, Bristol (1996).
- [2] NSNS Collaboration, “NSNS Conceptual Design Report.”– NSNS/CDR-2/V1, Oak Ridge, TN (1997).
- [3] J.S. Lundsford and R.A. Hardekopf, *IEEE Trans. NS*, **NS-30**, 2830 (1983).
- [4] S.S. Kurennoy, A.J. Jason, F.L. Krawczyk, and J.F. Power, in *Proceed. PAC97 (Vancouver, BC, 1997)*.
- [5] *MAFIA release 4.00*. – CST, Darmstadt, 1997.
- [6] W.J.R. Hoefer, *IEEE Trans. MTT*, **MTT-25**, 822 (1977).
- [7] S.S. Kurennoy, “Beam Chopper System for SNS”, Report LA-CP-98-156, Los Alamos (1998).
- [8] S.S. Kurennoy and J.F. Power, in *Proceed. LINAC98 (Chicago, 1998)*.